J. A. Felgueiras et al., Effect of blood viscoelastic property in hemodynamic simulations of carotid arteries, Revista Mecânica Experimental, No 33, APAET (2021), pp.39-50.

Effect of blood viscoelastic property in hemodynamic simulations of carotid arteries

Efeito da propriedade viscoelástica do sangue em simulações hemodinâmicas de artérias carótidas

J.A. Felgueiras[1] | L.C. Sousa[1,2] | C.C. António[1,2] | E. Azevedo[3,4] | C.F. Castro[1,2] | S.I.S. Pinto[1,2 (*)]

[1]Engineering Faculty, University of Porto, Porto, Portugal
[2]Institute of Science and Innovation in Mechanical and Industrial Engineering (LAETA-INEGI), Porto, Portugal
[3]Department of Neurology, Centro Hospitalar Universitário São João, Porto, Portugal
[4]Department of Clinical Neurosciences and Mental Health, Faculty of Medicine, University of Porto, Portugal
[(*)]*Email:* spinto@fe.up.pt

abstract

The study of the influence of the blood viscoelastic property in numerical simulations is still a challenge in the scientific community, mainly in patient-specific arteries with complex geometry. It is well-known from the literature that considering the viscoelastic property of blood is important in arteries with small calibre such as coronary arteries. However, as far as we know, it is not verified for arteries with medium calibre such as carotid arteries (≈ 8mm diameter). Thus, the novelty of the present work highlights the comparison of the hemodynamic descriptors when using the purely shear-thinning non-Newtonian model, Carreau model, and the viscoelastic non-Newtonian property of blood, multi-mode sPTTmodel, for the flow simulation in patient-specific carotid arteries. The differences are clearly notable in the bifurcation region with a 67% increase of the relative residence time when considering the viscoelastic model. Thus, it is evident that using the viscoelastic property of blood (sPTT model), so far the most realistic model, should be considered in arteries with large cross-sectional areas, such as carotid arteries.

Keywords: viscoelasticity, hemodynamic simulations, carotid arteries, atherosclerosis.

resumo

O estudo da influência da propriedade viscoelástica do sangue em simulações numéricas ainda é um desafio na comunidade científica, principalmente em artérias específicas de pacientes com geometria complexa. É bem sabido da literatura que a consideração da propriedade viscoelástica do sangue é importante em artérias de pequeno calibre como as coronárias. No entanto, até onde sabemos, não está comprovado para artérias de médio calibre, como as artérias carótidas (≈ 8 mm de diâmetro). Assim, a novidade do presente trabalho destaca a comparação dos descritores hemodinâmicos ao usar o modelo puramente pseudoplástico não-Newtoniano, modelo de Carreau, e a propriedade viscoelástica não-Newtoniana do sangue, modelo sPTT multimodo, para a simulação do fluxo em artérias carótidas específicas do paciente. As diferenças são claramente notáveis na região de bifurcação com um aumento de 67% do tempo de residência relativo quando considerado o modelo viscoelástico. Assim, fica evidente que o uso da propriedade viscoelástica do sangue (modelo sPTT), até ao momento o modelo mais realista, deve ser considerado em artérias com grandes áreas transversais, como as artérias carótidas.

Palavras-chave: viscoelasticidade, simulações hemodinâmicas, artérias carótidas, aterosclerose.

1- INTRODUCTION

Cardiovascular and cerebrovascular diseases have been, nowadays, one of the main causes of mortality in developed countries (Mozaffarian et al. 2015). Published research shows and clinical practice reinforces that specific locations in the human circulatory system, such as bifurcations and arterial curvatures, are susceptible to the development of cardiovascular diseases such as atherosclerosis – accumulation of fat substances, lipoproteins and calcium in the arterial wall - causing stenosis and diminishing or blocking the normal circulation of blood.

Individual hemodynamics analysis is an essential tool for the diagnosis and treatment of cardiovascular diseases. Ultrasound (US) Doppler images of carotid arteries can provide information on the geometry of the artery and on the location and degree of stenosis. Nevertheless, images alone do not explain in detail the hemodynamics.

A numerical tool to simulate blood flow, as close as possible the hemodynamics of a patient-specific carotid artery, is of extreme importance for better assistance in research and clinical practice. Several authors have advanced in this research field. Lee et al. (2012) have considered the influence of the fluid-structure interaction on hemodynamics in carotid artery based on patient-specific clinical data. Conti et al. (2016) have studied the carotid artery hemodynamics before and after stenting. This work incorporates a patient-specific CFD study. Azar et al. (2019) have conducted a retrospective study on pre-CEA computed tomography angiography images from several patients with severe stenosis (>60% stenosis) to better understand the influence of plaque and local vessel geometry on local hemodynamics, with geometrical descriptors that extend beyond the degree of stenosis. Authors of the present study have also been developing a hemodynamic numerical tool. The influence of geometric parameters of left and right coronary arteries in the atherosusceptibility of healthy patients were carried out using fluid-structure interaction for numerical simulations (Pinho et al. 2019a, Pinho et al. 2019b). However, none of the studies cited previously takes into account the most accurate rheology of blood. They have assumed blood as a Newtonian fluid or a purely shear-thinning fluid.

Recently, user-defined-functions (UDFs) in ANSYS® software have been implemented and validated, by the authors, to simulate specific conditions, assigning properties as close as possible to real blood properties, such as the viscoelastic property of blood (Bodnár et al. 2011, Campo-Deaño et al. 2013, Good et al. 2016, Romano et al. 2020a, Romano et al. 2020b, Pinto et al. 2020). It is well-known from previous studies of the authors (Romano et al. 2020a, Romano et al. 2020b, Pinto et al. 2020) that the viscoelastic property of blood, the Simplified Phan-Thien/Than (sPTT) model, is the most accurate and the most realistic to use in hemodynamic simulations of coronary arteries, arteries with cross-sectional areas lower than 4mm (small calibre).

As far as we know there are no studies simulating the hemodynamics in arteries with medium calibre, such as carotid arteries (≈ 8mm diameter), considering the viscoelastic property of blood. Thus, the goal of the present work is to verify if the use of this viscoelastic model in hemodynamic simulations of carotid arteries, arteries with larger cross-sectional areas, presents significant and different results than using a purely shear-thinning model such as Carreau model. Numerical results of the hemodynamic descriptors, such as the time averaged wall shear stress

(TAWSS), oscillatory shear index (OSI) and relative residence time (RRT), will be compared, in a patient-specific carotid artery with stenosis.

2- METHODOLOGY

Numerical simulations were carried out to study the influence of the viscoelastic property of blood in arteries with medium calibre such as carotid arteries. Therefore, a geometric model of a patient-specific artery was reconstructed and the computational mesh was generated. Inlet and outlet boundary conditions were imposed and properties of blood and arterial wall, used for numerical simulations, were highlighted. The numerical method was described and the wall shear stress hemodynamic descriptors were defined.

2.1. Geometry reconstruction

Geometric models of patient-specific carotid arteries were reconstructed through Femap® software, taking into account the bifurcation region of the common carotid artery (CCA), the internal carotid artery (ICA) and external carotid artery (ECA). The US Doppler images necessary for the reconstruction were obtained by the Department of Neurology of São João Hospital Center. These images were acquired by the use of a General Electric Healthcare Vivid ultrasound with an 8LR-RS linear probe (frequency 4 to 10 MHz). The 3D models were already reconstructed in previous works of the authors (Henriques 2015; Silva 2015). The one considered for this study has a 50% degree of stenosis in ICA, as can be seen in Figure 1.

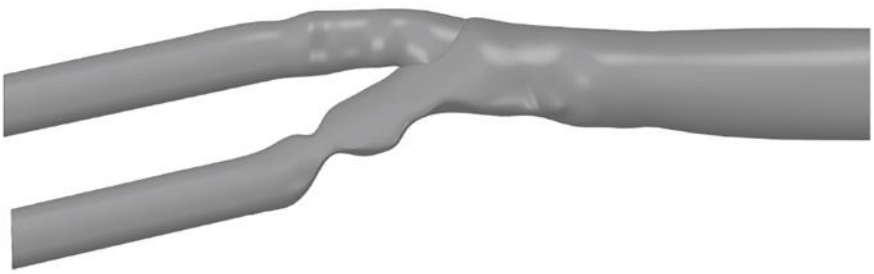

Fig. 1 | 3D patient-specific artery model with 50% degree of stenosis in ICA.

2.2. Computational mesh

The computational mesh was generated using Meshing Ansys®. Two parameters must be evaluated to attain a mesh with good quality elements and the most suitable to achieve accurate results. Tetrahedral elements were chosen to apply a method in order to uniform the elements and avoid agglomeration of elements, and consequent increase of elements number, in unnecessary regions.

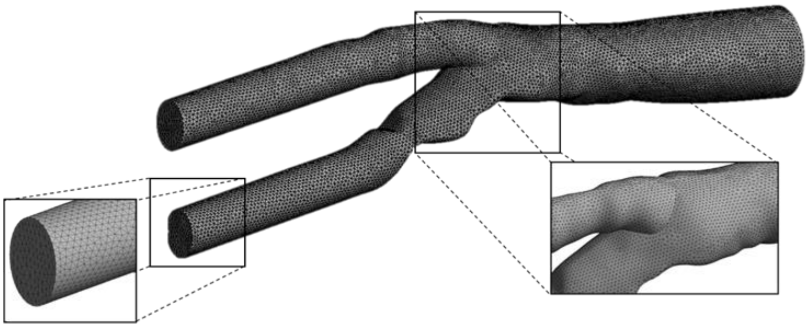

Fig. 2 | Tetrahedral computation mesh for the study case.

Thus, the quality of the mesh was evaluated through the statistical parameter Skewness. The Skewness determines the orthogonality of the mesh elements. An element with a Skewness higher than 0.95 (maximum value stipulated in Ansys® tutorial (Ansys Academic 16.0 2013) for this type of geometry) has poor quality. The Maximum Skewness must be lower than 0.95. In the present work, the Maximum Skewness obtained was 0.599 with an Average Skewness of 0.124 within all the elements. The majority of the elements has a Skewness near 0, meaning that almost all of the elements are equilateral forming a good mesh quality.

Then, mesh tests considering the viscoelastic property of blood (more complex property) were performed in order to assure the precision of the results. The TAWSS, OSI and RRT were achieved in function of the number of elements as can be seen in Figure 3. The most accurate mesh with the lost computational time on running simulations is the one where the plateau starts, for all the hemodynamic descriptors. Thus, following these criteria, a mesh with 1 468 927 elements was used.

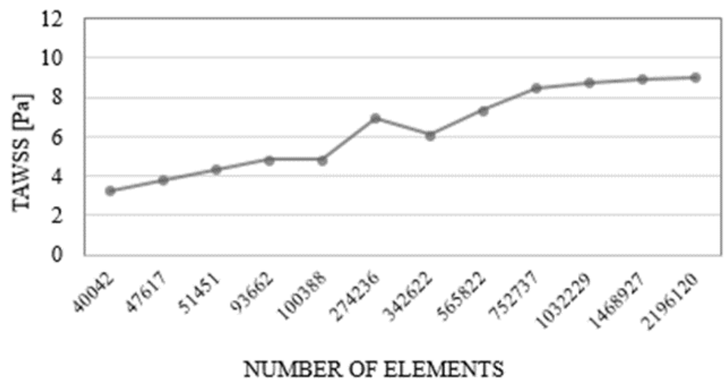

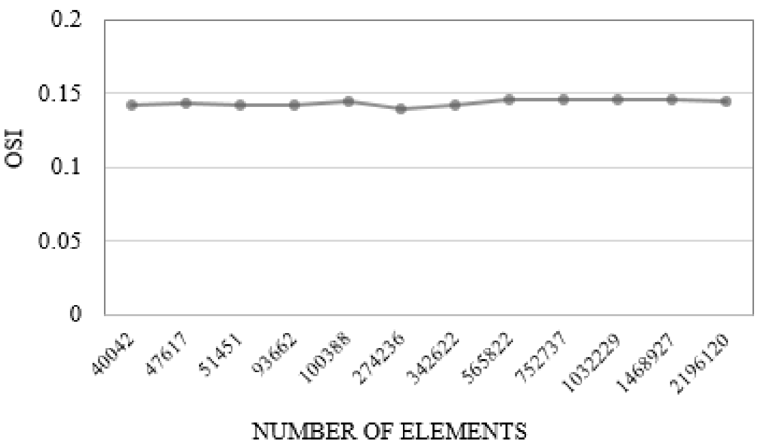

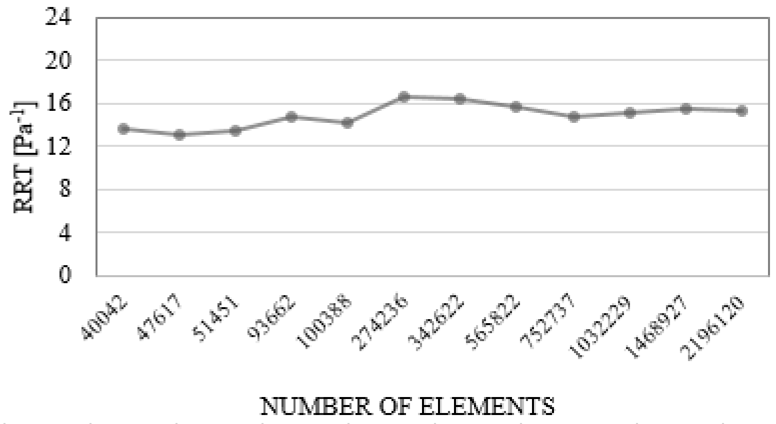

Fig. 2 | TAWSS, OSI and RRT vs. number of elements.

2.3. Boundary conditions

At the inlet of the CCA, a Womersley velocity profile was imposed:

$$v(r_d, t) = \frac{A \cdot R^2}{i \cdot \mu_f \cdot \alpha^2} \times \left[1 - \frac{J_0\left(i^{3/2} \cdot W_o \cdot \frac{r_d}{R}\right)}{J_0\left(i^{3/2} \cdot W_o\right)}\right] \cdot e^{i\omega t} \tag{1}$$

where r_d corresponds to the radial distance between the center of the artery and a radial point, $A = \frac{1}{\rho}\frac{\partial P}{\partial rd}$ is the pressure gradient, R is the radio of the artery, μ_f is the dynamic viscosity of blood, J_0 is the first order function of Bessel, ω is the cardiac frequency of the patient and W_o is the Womersley number, defined by:

$$W_o = R\sqrt{\frac{\rho\omega}{\mu_f}} \tag{2}$$

For this specific case of an artery with a diameter of 7.8 mm and cardiac frequency equal to 8.2 Hz, the Womersley number is 6.19. Since this number is higher than 1, it is important to highlight that Poiseuille profile is not sufficient. Thus, the Womersley velocity profile was implemented by the authors in a user-defined function (UDF) of Ansys® software (Ferreira 2013).

At the outlets of ICA and ECA, a flow rate distribution of 50/50 was imposed. In previous works, local numerical velocities (from computational simulations) were compared with local velocities from US images of this patient (Gonçalves 2014, Khalafvand & Han 2015); and the flow rate distribution ICA/ECA which best fits this comparison is 50/50.

2.4. Blood and arterial wall properties

Blood has been considered as an isotropic, incompressible and non-Newtonian fluid with constant density equal to 1060 kg/m³. Carreau model, representing the shear-thinning property of blood, is the most used by other authors (Lee et al. 2012, Azar et al. 2019):

$$\mu = \mu_\infty + (\mu_0 - \mu_\infty)[1 + (\lambda_C \dot{\gamma})^2]^{(n_c - 1)/2} \tag{3}$$

where μ_∞ represents the viscosity when the shear rate ($\dot{\gamma}$) tends to infinite and μ_0 reports the zero shear viscosity. λ_C is the relaxation time and n_c the characteristic constant of the flow. The respective values for human blood at 37ºC are represented in Table 1 (Johnston et al. 2004).

However, blood is a very complex fluid constituted by several cellular elements and plasma. It is well-known from the literature that blood has a non-Newtonian viscoelastic behavior (Bodnár et al. 2011, Campo-Deaño et al. 2013, Good et al. 2016, Romano et al. 2020a, Romano et al. 2020b, Pinto et al. 2020), mainly in arteries with low calibre. Authors of the present paper have implemented viscoelastic models for blood in UDFs of Ansys® software, for studies of coronary arteries – arteries with low calibre (Romano et al. 2020a, Romano et al. 2020b, Pinto et al. 2020, Miranda et al. 2021). Several constitutive models constitutive models were employed such as Oldroyed-B, multi-mode Giesekus and multi-mode Simplified Phan-Thien/Tanner (sPTT). Although the last two models present the same results (Pinto et al. 2020), the multi-mode sPTT model is the preferential option for this application, since Giesekus model introduces the second normal stress difference, which so far has not been reported for blood.

Table 1 | Values of Carreau model for human blood at 37ºC (Johnston et al. 2004).

Parameters	Constant values
μ_0	0.0560 Pa.s
μ_∞	0.00345 Pa.s
λ_C	3.313 s
n_c	0.3568

Mathematically, the total force ($\boldsymbol{\tau}$) is expressed as the sum of the solvent ($\boldsymbol{\tau}_s$) and the elastic ($\boldsymbol{\tau}_e$) contributions, as an analogue to the decomposition of the stress tensor $\boldsymbol{\tau}$:

$$\boldsymbol{\tau} = \boldsymbol{\tau}_s + \boldsymbol{\tau}_e \tag{5}$$

where $\boldsymbol{\tau}_s$ depends on the viscosity of the solvent (μ_s) and on the strain rate tensor ($\mathbf{D}$):

$$\tau_s = 2\mu_s\mathbf{D} \tag{6}$$

and, for multi-mode sPTT model, $\boldsymbol{\tau}_e$ depends on the relaxation time (λ_k), the elastic viscosity ($\mu_{(e_k)}$) and the upper-convected derivative ($\overset{\nabla}{\boldsymbol{\tau}}_{e_k}$) of each mode k:

$$f(\boldsymbol{\tau}_{e_k})\boldsymbol{\tau}_{e_k} + \lambda_k \overset{\nabla}{\boldsymbol{\tau}}_{e_k} = 2\mu_{e_k}\mathbf{D} \tag{7}$$

The sum of the elastic stress of each k mode ($\boldsymbol{\tau}_{e_k}$), in the total of m modes, allows to express the total elastic stress ($\boldsymbol{\tau}_e$):

$$\boldsymbol{\tau}_e = \sum_{k=1}^{m} \boldsymbol{\tau}_{e_k} \tag{8}$$

The values of the multi-mode sPTT model for human blood were obtained experiment-tally by Campo-Deaño et al. (2013) and are represented in Table 2. These values are the inputs of our implemented model in UDFs of Ansys®.

Although the arterial wall deforms along the cardiac cycle, the arterial wall was considered rigid for this study. In fact, it was reported by Miranda et al. (2021) that the result differences considering rigid or deformable wall are insignificant and the computational time when deformable walls are taken into account is 48 times higher. Thus, using a deformable wall is not compensatory.

Table 2 | Values of multi-mode sPTT model for human blood (Campo-Deaño et al. 2013).

Mode	μ_{e_k}(Pa.s)	λ_k(s)	ε_k
1	0.05	7	0.2
2	0.001	0.4	0.5
3	0.001	0.04	0.5
4	0.0016	0.006	0.5
Solvent	μ_s = 0.0012 (Pa.s)		

2.5. Numerical method

The numerical simulations were performed in Fluent Ansys®. The computational fluid dynamics model was set up for unsteady flow due to the time-dependent nature of the models at hand. At each time step, 5×10^{-3}s, the velocity-pressure coupled equations were solved with the SIMPLE algorithm. The momentum and constitutive equations were discretized by the second order upwind scheme. A convergence criterion of 1×10^{-4} was used. The numerical method is the same of previous works using patient-specific coronary arteries and the validation was already carried out (Romano et al. 2020a, Romano et al. 2020b, Pinto et al. 2020).

2.6. Wall shear stress hemodynamic descriptors

The most used wall shear stress (WSS) hemodynamic descriptors to describe the blood flow behavior in patient-specific arteries are the Time-Averaged Wall Shear Stress (TAWSS), the Oscillatory Shear Index (OSI) and the Relative Residence Time (RRT). Through these hemodynamic descriptors, some authors have associated the low WSS magnitude with the flow disorder, in order to predict the probability of the atherosclerosis appearance in arteries (Malek et al.1999; Tarbell 2003).

TAWSS determines the mean value of the WSS magnitude along the cardiac cycle:

$$\mathrm{TAWSS} = \frac{1}{T}\int_0^T |\mathbf{WSS}(\boldsymbol{s},\boldsymbol{t})| \cdot \mathrm{d}t \tag{9}$$

T represents the total time of the cardiac cycle, s is the location in the arterial wall and t the instant time. The tendency to appear atherosclerotic plaque is higher when TAWSS is lower than 0.4 Pa (Malek et al. 1999).

OSI evaluates the arterial wall regions where the directional flow changes occur:

$$\mathrm{OSI} = \frac{1}{2}\left[1 - \left(\frac{\int_0^T |\mathbf{WSS}(s,t)| \cdot dt}{\int_0^T \mathbf{WSS}(s,t) \cdot dt}\right)\right] \tag{10}$$

The atherosclerotic plaque formation is more susceptible in regions where OSI is higher than 0.25 to a maximum of 0.5 (He & Ku 1996).

RRT indicates the residence time of the particles near the wall. This descriptor is directly proportional to OSI and inversely to TAWSS (Gallo et al. 2014):

$$\mathrm{RRT} = \frac{1}{(1-2 \cdot OSI) \cdot TAWSS} \tag{11}$$

RRT can vary from 0 to infinity. The atherosusceptible regions occur when RRT value is higher than 8 Pa^{-1}.

3- RESULTS AND DISCUSSION

Figures 4, 5 and 6 show the TAWSS, OSI and RRT spatial distribution, in the patient-specific carotid artery, for assessing the tendency of atherosusceptibility. In each figure, the results in front and back views are represented, as well as the results using the purely shear-thinning property of blood (Carreau model) and considering the viscoelastic property of blood (sPTT model) in the simulations.

Regarding Figure 4, TAWSS is near 0 Pa, most critical regions for atherosusceptibility, along the main artery of CCA, in the bifurcation and before and after the stenosis in ICA. These regions are even more emphasized when multi-mode sPTT is used instead of Carreau model for simulations. In the main artery of CCA, a maximum TAWSS of 0.3 Pa for sPTT model and a value of 0.9 Pa for Carreau model can be observed. Moreover, in the bifurcation region, the maximum value of TAWSS is 0.03 Pa for sPTT and 0.25 Pa for Carreau. In the stenotic region, there is a maximum

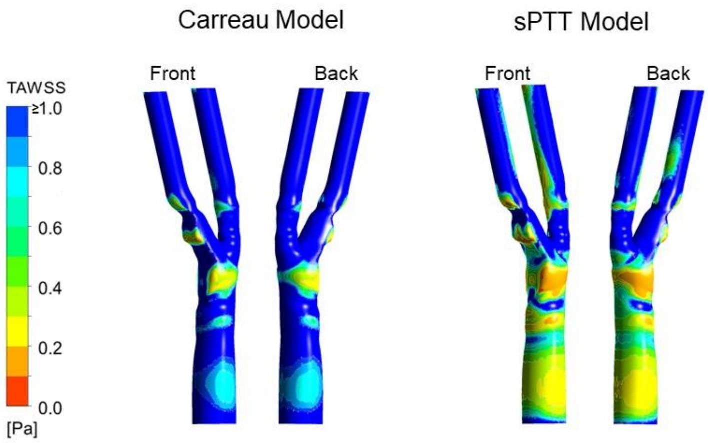

Fig. 4 | TAWSS for the patient-specific carotid artery using Carreau model and multi-mode sPTT model, for numerical simulations

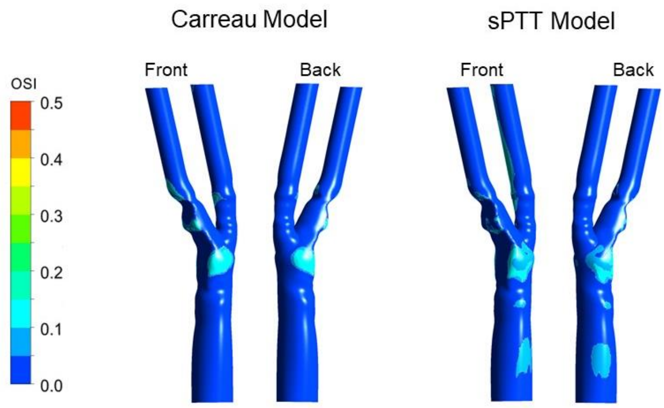

Fig. 5 | OSI for the patient-specific carotid artery using Carreau model and multi-mode sPTT model, for numerical simulations

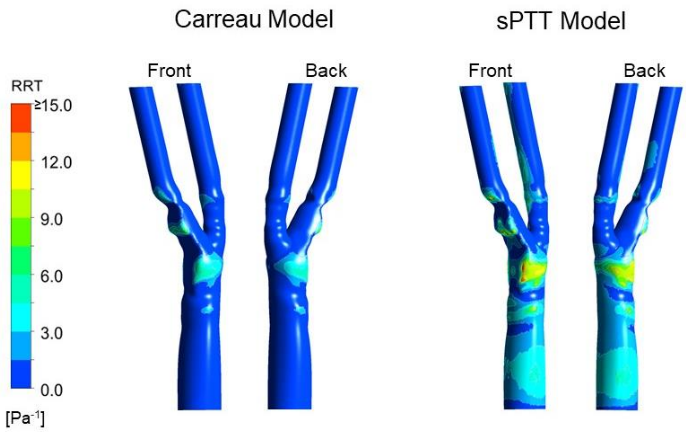

Fig. 6 | RRT for the patient-specific carotid artery using Carreau model and multi-mode sPTT model, for numerical simulations

value of TAWSS of 0.01 Pa for sPTT and 0.15 Pa for Carreau. The differences between using the viscoelastic model (multi-mode sPTT) and the purely shear-thinning model (Carreau) are significant in hemodynamic simulations in a CCA with a diameter of 7.8mm.

Concerning Figure 5, OSI is higher in the bifurcation region, presenting values of 0.15 considering both models. In these regions, there are more directional flow changes than in the other areas, although with low values. As indicated by the literature, this descriptor is the one that less describes the susceptible regions to atherosclerosis appearance (Lee et al. 2009, Pinto et al. 2019a).

Figure 6 represents RRT, the strongest hemodynamic descriptor (Knight et al. 2010), which combines TAWSS and OSI. As TAWSS descriptor, the most atherosusceptible regions can be detected in the main artery of the CCA, in the bifurcation and in the stenotic region in ICA. These regions are more critical when multi-mode sPTT model is used instead of Carreau model. In the main CCA, the maximum RRT value is 4 Pa^{-1} for sPTT model and near 0 for Carreau model. Futhermore, in the bifurcation, the maximum RRT is higher than 15 Pa^{-1} for sPTT model and is 5 Pa^{-1} for Carreau model. In the stenotic region in ICA, the maximum RRT is 9 Pa^{-1} for sPTT model and 8 Pa^{-1} for Carreau. Thus, significant differences in RRT results can be enhanced when the viscoelastic model (multi-mode sPTT) and the purely shear-thinning model (Carreau model) are used for hemodynamic simulations in arteries with medium calibre, such as carotid arteries.

4- CONCLUSION

Based on US Doppler images provided by the medical team, a 3D geometry of CCA with a 50% stenosis located in ICA was constructed through Femap® software. Then, Ansys® software, coupled with implemented UDFs, was used to construct the mesh and perform the hemodynamic simulations. Two different methodologies for hemodynamic simulations were considered, one of them using the purely shear-thinning property of blood (Carreau model) mainly used by several authors (Lee et al. 2012, Conti et al. 2016, Azar et al. 2019) and another considering the viscoelastic property of blood (sPTT model). It is well-known from the literature that blood is viscoelastic (Bodnár et al. 2011, Campo-Deaño et al. 2013, Good et al. 2016, Romano et al. 2020a, Romano et al. 2020b, Pinto et al. 2020). However, the implementation of these constitutive equations is complex and the computational time is higher. This is the reason that many authors have opted for the shear-thinning non-Newtonian model (simpler model). However, in arteries with small calibre such as coronary arteries, this is not the best option since viscoelastic property significantly changes the results (Romano et al. 2020a, Romano et al. 2020b, Pinto et al. 2020, Miranda et al. 2021). In the present work, it was concluded that the viscoelasticity of blood also affects results in arteries with medium calibre, such as carotid arteries (arteries with 8 mm diameter). Differences using the purely shear-thinning model and the viscoelastic model for the hemodynamic simulations of carotid arteries are clearly notable. Considering the sPTT model, there is an RRT increase of 67% in the bifurcation (highest increase), an increase of 33% in the main branch of CCA and an increase of 11% in the stenotic region of ICA. The computational time is also 5 times higher but the results are more accurate. These specific hemodynamic descriptors values depend on the particular geometry of the carotid artery and are according to the clinical practice, where the most propitious regions for atherosclerosis appearance are in CCA and ICA.

ACKNOWLEDGMENTS

Authors gratefully acknowledge the financial support by FCT, Portugal, the Engineering Faculty of University of Porto, the Institute of Science and Innovation in Mechanical and Industrial Engineering, the Department of Clinical Neurosciences and Mental Health of the Medicine Faculty of University of Porto and the Department of Neurology of *Centro Hospitalar Universitário São João*, Porto.

REFERENCES

Ansys Academic 16.0. ANSYS Fluent Tutorial Guide, Ansys ®, 2013.

A.M. Malek, S.L. Alper, S. Izumo. Hemodynamic shear stress and its role in atherosclerosis. J Am Med Assoc. 282:2035–2042, 1999.

B.C. Good, S. Deutsch., K.B. Manning. Hemodynamics in a pediatric ascending aorta using a viscoelastic pediatric blood model. Ann. Biomed. Eng., 44:1019-1035, 2016.

B.M. Johnston, P.R. Johnston, S. Corney, D. Kilpatrick. Non-Newtonian blood flow in human right coronary arteries: Steady state simulations. Journal of Biomechanics, 131: 709–720, 2004.

D. Azar, W.M. Torres, L.A. Davis, T. Shaw, J.F. Eberth, V.B. Kolachalama, S.M. Lessner, T. Shazly. Geometric determinants of local hemodynamics in severe carotid artery stenosis. Comput Biol Med 114: 103436, 2019.

D. Gallo, G. Isu, D. Massai, F. Pennella, M.A. Deriu, R. Ponzini, C. Bignardi, A. Audenino, G. Rizzo, U. Morbiducci. A survey of quantitative descriptors of arterial flows. Vis Simul Complex Flows Biomed Eng. Dordrecht. 1–24, 2014.

D. Mozaffarian, E.J. Benjamin, A.S. Go et al. Heart disease and stroke statistics. Circulation, 131: 29-322, 2015.

E. Miranda, L.C. Sousa, C.C. António, C.F. Castro, S.I.S. Pinto. Role of the left coronary artery geometry configuration in atherosusceptibility: CFD simulations considering sPTT model for blood, 1-16, 2021.

E. Romano, L.C. Sousa, C.C. António, C.F. Castro, S.I.S. Pinto. Non-Linear or quasi-linear viscoelastic property of blood for hemodynamic simulations, In Developments and Novel Approaches in Biomechanics and Metamaterials, Advanced Structured Materials, 132:127-139, 2020.

E. Romano, L.C. Sousa, C.C. António, C.F. Castro, S.I.S. Pinto, WSS descriptors in a patient RCA taking into account the non-linear viscoelasticity of blood, In Developments and Novel Approaches in Biomechanics and Metamaterials, Advanced Structured Materials, 132: 141-152, 2020.

H.A. Henriques. Caracterização do fluxo sanguíneo duma Bifurcação da Artéria Carótida com Estenose, 2015.

H.J. Silva. Caracterização do fluxo sanguíneo duma Bifurcação da Artéria Carótida com Estenose, 2015.

J. Knight, U. Olgac, S.C. Saur, D. Poulikakos, W. Marshall, P.C. Cattin, H. Alkadhi, V. Kurtcuoglu. Choosing the optimal wall shear parameter for the prediction of plaque location – A patient-specific computational study in human right coronary arteries. Atherosclerosis, 211: 445-450, 2010.

J.M. Tarbell. Mass transport in arteries and the localization of atherosclerosis. Annu Rev Biomed Eng. 5:79–118, 2003.

J. P. R. Gonçalves. Cirurgia Virtual de Próteses Arteriais, 2014.

L. Campo-Deaño, R.P.A. Dullens, D.G.A.L. Aarts., F.T. Pinho, M.S.N. Oliveira. Viscoelasticity of blood and viscoelastic blood analogues for use in polydymethylsiloxane in vitro models of the circulatory system. Biomicrofluidics, 7: 34102, 2013.

M. Conti, C. Long, M. Marconi, R. Berchiolli, Y. Bazilevs, A. Reali. Carotid artery hemodynamics before and after stenting: A patient specific CFD study. Computers and Fluids 141:62-74, 2016.

M. C. Ferreira, Estudo Hemodinâmico da Bifurcação da Artéria Carótida tendo em vista aplicação hospitalar. 2013

N. Pinho, C.F. Castro, C.C. António, N. Bettencourt, L.C. Sousa, S.I.S Pinto. Correlation between geometric parameters of the left coronary artery and hemodynamic descriptors of atherosclerosis - FSI and statistical study. Medical & Biological Engineering & Computing, 57: 715-729, 2019.

N. Pinho, L.C. Sousa, C.F. Castro, C.C. António, C. Carvalho, W. Ferreira, R. Ladeiras-Lopes, N.D. Ferreira, P. Braga, N. Bettencourt, S.I.S. Pinto. The impact of the right coronary artery geometric parameters on hemodynamic performance. Cardiovascular Engineering and Technology, 10:257-270, 2019.

S.H. Lee, S. Kang, N. Hur, S.K. Jeong. A fluid-structure interaction analysis on hemodynamics in carotid artery based on patient-specific clinical data, Journal of Mechanical Science and Technology 26:1-11, 2012.

S.I.S. Pinto, E. Romano, C.C. Antonio, L.C. Sousa, C.F. Castro. The impact of non-linear viscoelastic property of blood in right coronary arteries hemodynamics – A numerical implementation. International Journal of Non-Linear Mechanics, 123: 1-14, 2020.

S.S. Khalafvand and H.C. Han. Stability of Carotid Artery Under Steady-State and Pulsatile Blood Flow: A Fluid-Structure Interaction Study. Journal of Biomechanical Engineering, 6: 1–8, 2015.

S. W. Lee, L. Antiga, and D. A. Steinman. Correlations among indicators of disturbed flow at the normal carotid bifurcation. Journal of Biomechanical Engineering, 131: 1–7, 2009.

T. Bodnár, A. Sequeira, M. Prosi. On the shear-thinning and viscoelastic effects of blood flow under various flow rates. Appl. Math. Comput, 217: 5055-5067, 2011.

X. He, D.N. Ku. Pulsatile flow in the human left coronary artery bifurcation: Average conditions. J Biomech Eng. 118:74–82, 1996.